Corrosion behavior of Sn-9Zn-xBi lead-free solder alloys in NaCl 3% solution

Adnane Ahmido[1], Souad El Hajjaji[1]*, Benaceur Ouaki[3], A.Sabbar[2], Saloua Sebbahi[1]

[1]Laboratoire de Spectroscopie, Modélisation Moléculaire, Matériaux et Environnement, Faculté des Sciences, Université Med V, Av.Ibn Battouta, B.P.1014, M-10000 Rabat, (MAROC)
[2]Equipe de Physico-Chimie des Matériaux et Nanomatériaux : Environnement, Dépollution et Développement Durable, Faculté des Sciences, Université Med V Agdal, Av.Ibn Battouta, B.P.1014, M-10000 Rabat, (MAROC)
[3]Département de Génie des Matériaux, Ecole Nationale de L'Industrie Minérale Rabat, (MAROC)
E-mail: selhajjaji@hotmail.com

ABSTRACT

Corrosion behavior of Sn–9Zn-xBi alloys (x=0; 0.5 and 3 wt%) were studied in NaCl 3% solution using open circuit potential, polarization curves, weight loss measurements and surface analysis. The obtained results revealed the corrosion resistance depends on the percentage of bismuth. The Sn-9Zn-3Bi has the lowest values of corrosion current density. The corrosion potential shift toward more negative values with more bismuth addition. XRD analysis of the corrosion products formed after 168 hours of immersion in NaCl 3% solution indicated the zinc dissolution.
© 2015 Trade Science Inc. - INDIA

INTRODUCTION

The binary Sn–Pb alloys have long been used in the microelectronic packaging industry. However, for the lead toxicity and his serious effects on the environment and human health, it has been prohibited in all are[1]. Many Sn-based alloy systems (Pb-free solder alloy) with different alloying elements, such as Ag, In, Cu, Zn, Bi and Sb have been developed and their microstructures, mechanical properties and solderability have been reported[2-13]. Among this alloys, the Sn–9Zn (in wt%) alloy is considered as a potential candidate and has attracted great attentions because of its low cost and good mechanical properties. Indeed, it has a melting point (198.5 °C) very close to conventional Sn–37 wt% Pb alloy

(183 °C)[14, 15]. Despite these advantages, Sn–Zn alloys suffer from low oxidation resistance[1] and poor wettability[1, 16]. Bismuth has been added to the binary Sn–Zn alloy to form the ternary eutectic Sn–8Zn–3Bi, with improved wettability[17, 18], lower melting point of 188°C[19] and better mechanical properties[20].

However, there is a lack of information about electrochemical behavior of Sn-9Zn-xBi in NaCl solution. The objectives of this study is to investigate the effect of the addition of small amounts of Bi (x=0; 0.5 and 3 wt%) to Sn-9Zn alloy on its corrosion resistance in NaCl 3wt% solution using electrochemical methods such as potentiodynamic polarisation techniques and weight loss measurements. Finally, the mechanism of corrosion will be

Full Paper

discussed from electrochemical results and XRD analysis.

EXPERIMENTAL PROCEDURE

Materials preparation

The alloys were prepared from high-purity 5N metals. For each alloy, the metals (Sn, Zn and Bi) were weighted and sealed into Pyrex capsules under vacuum and melted together at 350 °C. After several days of heat treatment, the alloys were quenched in ice water and used for our experiments. Chemical compositions of samples are given in TABLE 1.

Electrochemical investigation

The measurements were carried out in a conventional three electrode cylindrical glass cell, containing 100 mL of NaCl 3% solution at room temperature. Platinum electrode was used as a counter electrode, a saturated calomel electrode (SCE) as the reference electrode and the working electrode was Sn-9Zn-xBi alloy. All potentials are reported vs. SCE. For polarization measurements, a potentiostat Voltalab 301 PGZ monitored by a PC computer and Voltamaster 4.0 software were used

for run the tests, collect and evaluate the experimental data. During each experiment, the test solution was mixed with a magnetic stirrer.

Before every run, the surface of the electrode was polished using 600–1000 SiC paper grade, degreased with ethanol, washed in distilled water. The specimen was then dried in hot air and placed in the test cell. The tested solution was mixed with a magnetic stirrer. Before each Tafel experiment, the working electrode was allowed to corrode freely and its open circuit potential (OCP) was recorded as a function of time up to 1 h. After this time, a steady-state OCP, corresponding to the corrosion potential (Ecorr) of the working electrode, was obtained. The polarisation curves of alloys were recorded in the anodic direction from "2000 to +1000 mV at a scan rate of 2 mV/s.

RESULTS AND DISCUSSION

Electrochemical behavior

The open circuit potential (OCP) against time (Eocp – t) curves of the studied Pb-free solder alloys measured in NaCl 3 wt.% solution are shown in Figure 1.

TABLE 1 : Chemical compositions of the studied lead-free solder alloys (wt.%)

Alloy	Sn	Zn	Bi
Sn-9Zn	91	9	-
Sn-9Zn-0.5Bi	90.5	9	0.5
Sn-9Zn-3Bi	88	9	3
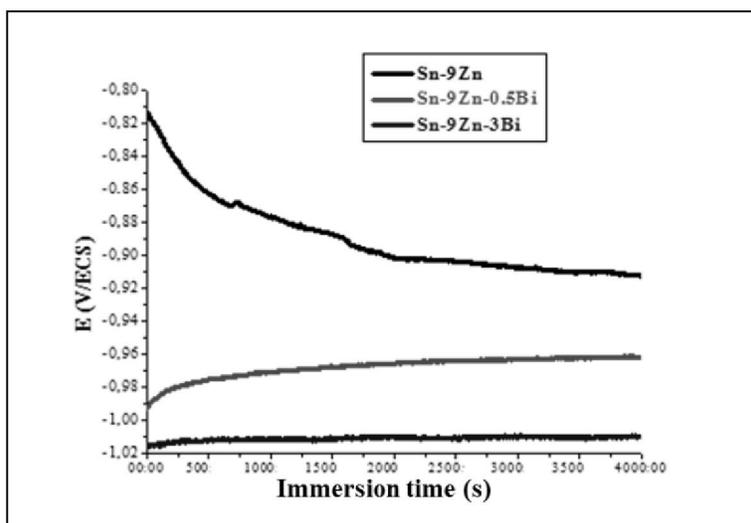
Figure 1 : OCP curves of the three studied alloys after an hour of immersion in NaCl 3% solution

The OCP of Sn–9Zn decrease quickly and then, an approximate constant values of E_{OCP} was obtained. The initial decrease of the OCP can be attributed to the strong removal of the natural oxide layer on the alloy surface. The OCP of Sn-9Zn-0.5Bi and Sn–9Zn–3Bi increases until to reach stationary state, which corresponds respectively to a value of -962 and"1009 mV/SCE. Such curves appearance is attributed to the ennoblement of the potential of the two electrodes. The existence of a plateau region for the OCP suggests that the alloys surfaces are completely covered by the corrosion product after about 500 s of immersion. The constant E_{OCP} obtained are very negative and reveal that the corrosive behavior of the three solder alloys is very similar to that

of pure Zn[21, 22]. The OCP curves of the three elements constituent of Pb-free solders Figure 2, tested in the same previous conditions, show that potential field of pure zinc correspond approximately to the potential range of the three alloys seen in Figure 1.

Figure 3 present the polarization curves of the three alloys tested in NaCl 3% solution between -2000 and 1000 mV/ECS.

The three Pb-free solder alloys indicate similar profiles, which exhibit two pseudo passivity platforms at anodic regions. Those curves show that the corrosion potential (E_{corr}) shift toward more negative values after addition of a small amount of bismuth (x=0.5 and 3 wt.%) to the eutectic Sn-9Zn. We can also declare that the progressive addition of bis-
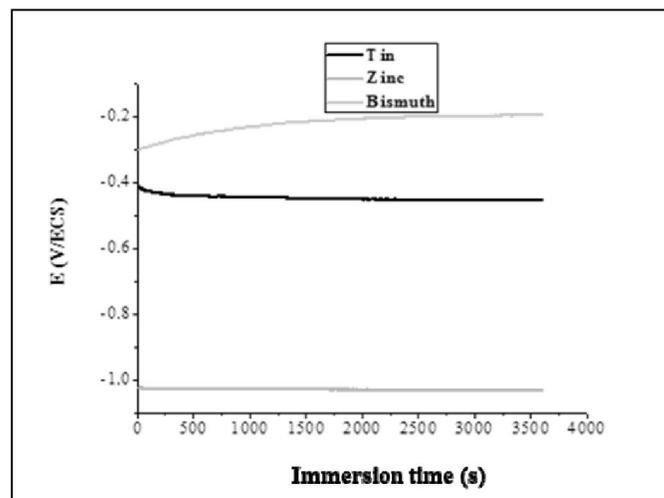
Figure 2 : OCP curves of pure tin, zinc and bismuth after an hour of immersion in NaCl 3% solution
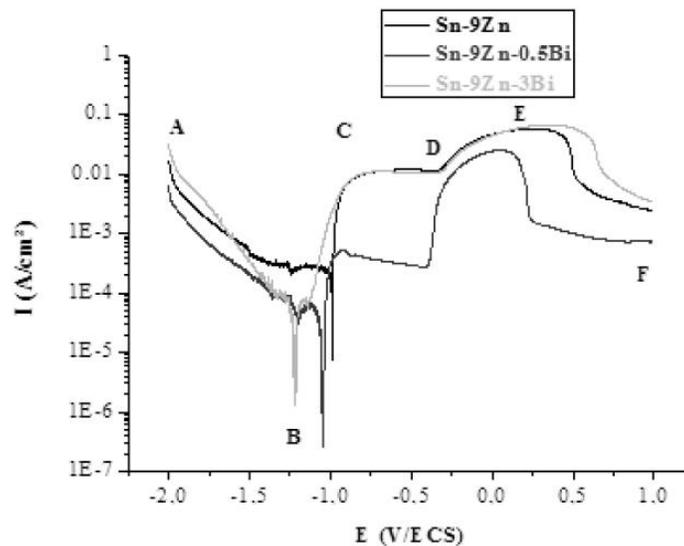
Figure 3 : Polarization curves of the studied solder alloys in NaCl 3 wt.% solution

Full Paper

TABLE 2 : Corrosion parameters obtained from electrochemical measurements (polarization curves) of solder alloys in NaCl 3 wt.% solution at room temperature

Alloys	E_{corr} (mV/ECS)	I_{corr} (µA/cm²)
Sn-9Zn	-984	262
Sn-9Zn-0.5Bi	-1041	66
Sn-9Zn-3Bi	-1229	61

muth induce a reduction the corrosion current density (I_{corr}) as shown in TABLE 2.

The cathodic reaction (region AB) may correspond to the reduction of oxygen in water resulting in the formation of hydroxyl ion.

$$2H_2O + O_2 + 4e^- \leftrightarrow 4\ OH^- \qquad (1)$$
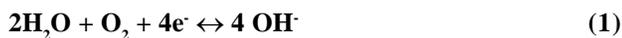
The anodic polarization part consists of several regions, named BC, CD, DE, and EF, respectively. At region BC, with increasing potential in the anodic direction, zinc dissolution occurs according to Eq. (2)[23].

$$Zn + 2OH^- \rightarrow Zn(OH)_2 \rightarrow ZnO + H_2O \qquad (2)$$

The first oxidation reaction produces $Zn(OH)_2$, and the second oxidation reaction transforms $Zn(OH)_2$ into ZnO. For Sn-9Zn-3Bi solder, active dissolution of zinc continues with increasing potential until the zincate concentration reaches a critical value (at point C). These insoluble zincate salts cover the surface of the corroded samples and create a plateau region (CD) where the current density is found to be independent of potential over a range of about 550 mV. This plateau can only be observed for the Sn-9Zn and Sn-9Zn-3Bi solder. The zinc oxidation film formed in region CD is not a passivation film; it cannot protect the solder from further corrosion[24]. Now it is generally accepted that the formation of the passivation film begins with precipitation of $Zn(OH)_2$ on the surface. After further corrosion, $Zn(OH)_2$ may transform into ZnO according to Eq. (2). ZnO is considered to be a semiconductor; it may degrade the corrosion resistance[25]. Thus, ZnO is harmful to the formation of the passivation film. The polarization curve of Sn-9Zn-0.5Bi shows that the current density does not remain constant in region CD. The formation of the passivation film on the solder starts at point C, where the current density drops as the potential increases. Region CD represents the passivation process of the solder. In this situation, the corrosion rates of the solders declined.

A sharp increase in current density is observed at point D on increasing the potential, indicating that the passivation film is broken. The breakdown of the passivation film can be caused both by the existence of Cl⁻ absorbed by the corrosion products and by the oxygen evolution reaction described above. From Eq. (1) the solution is alkaline during the test. It is difficult for metal to form a passivation film in alkaline solution. Furthermore, halogen, especially Cl⁻, can restrict passivation film formation. Chloride ions penetrate into the oxide film and form solid metal chloride, which causes mechanical breakdown of the film[26]. Halide ions stimulate active dissolution of zinc and result in breakdown of the passivation film[27]. $SnCl_2$ is able to absorb O_2 from air to form insoluble oxychloride, which is also harmful to the passivation film[28]. At point E, the curves line shift toward lower values until point F, which may represent a new process of passivation.

We have studied the polarization curves of the three elements constituent of alloy (Tin, Zinc and Bismuth) taking separately to give us an interpretation to the corrosion parameters of our alloys tested, as seen in Figure 4. We notice that the lowest and highest values correspond respectively to the corrosion potential and corrosion current density of Zinc (TABLE. 3), which are relatively compatible with the results obtained in TABLE. 2. TABLE. 3 inform us that Tin have the best corrosion resistant in NaCl 3%.

The anodic polarization of pure zinc was conducted to better understand the corrosion behavior of deposits in 3% NaCl solution. A typical anodic polarization curve part for pure zinc is shown in Figure 4. This curve has two regions. The first consists of active dissolution (from Ecorr to point A) of zinc and zinc dissolution continues with increasing potential until zinc hydroxy-chloride (ZHC) forms and covers the surface (point A). Many authors have
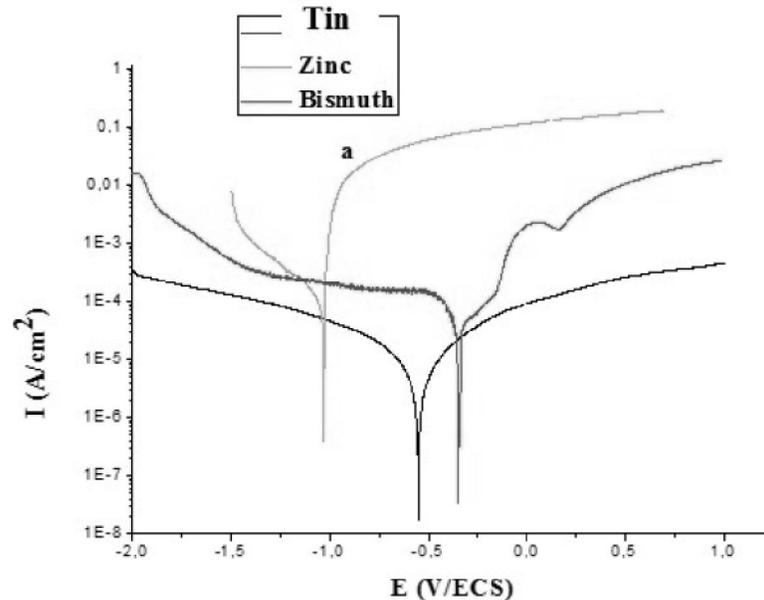
Figure 4 : Polarization curves of the studied solder alloys in NaCl 3 wt.% solution

TABLE 3 : Corrosion parameters obtained from electrochemical measurements (polarization curves) of pure metal in NaCl 3 wt.% solution

Pure metal	E_{corr} (mV/ECS)	I_{corr} (µA/cm²)
Tin	-567	31.64
Zinc	-1033	136
Bismuth	-348	121

reported that ZHC can be formed on the zinc surface during immersion in NaCl solution[29, 30, 31]. The ZHC layer formed in NaCl solution at pH<7 (acidic media) was porous[32], the ZHC layer can be classified as a pseudo-passive layer[33]. From point A, the pseudo-passive layer (ZHC) is formed on the zinc surface and the zinc dissolution continues, but the rate decreases[34].

When metal passivation occurs, the current density drops, as the potential increases[35]. Although there is an increase in potential, shown in Figure 4, the current density does not drop. The same behavior was observed of pure zinc in a 0.5 mol dm³ NaCl solution[36]. It is evident that in NaCl solution, a passive layer does not form, but it forms a zinc hydroxychloride, which is a pseudo-passive layer. When the whole sample surface is covered by this layer the rate of zinc dissolution decreases.

Weight loss measurement and surface analysis

The corrosion rates and surface analysis of the studied alloys after an immersion in NaCl 3wt.%

solution at room temperature for 168H are respectively shown in TABLE 4 and Figure 5. XRD analysis allows to determinate the probable corrosion products formed on the surface of each alloy (Figure 5), which point out a Zinc dissolution and the formation of ZnO and $Zn_5(OH)_8Cl_2H_2O$.

The corrosion behavior of Zinc in NaCl solution have been reported in several studies[37, 38, 39]. Corrosion of zinc begins with the oxidation of zinc at anodic sites (3)

$$Zn(s) \rightarrow Zn^{2+} + 2e\text{-} \qquad (3)$$

Zinc oxidation is balanced by a reduction reaction at cathodic sites; in aqueous corrosion environments typically the reduction of dissolved oxygen (4)

$$\tfrac{1}{2} O_2 + H_2O + 2e\text{-} \rightarrow 2OH^- \qquad (4)$$

It can be expected that the zinc cation and hydroxide anion react to produce zinc hydroxide or zinc oxide. The overall reaction is given by (5)

$$Zn^{2+} + \tfrac{1}{2} O_2 + H_2O \rightarrow Zn(OH)_2 \ (s)$$
$$\rightarrow ZnO(s) + H_2O \qquad (5)$$
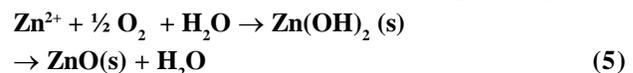
Full Paper

TABLE 4 : Corrosion rates measures of the three alloys after an immersion in NaCl 3% for 168 hours

	Weight loss (g)	Surface (cm²)	Immersion times (h)	Corrosion rates (g/cm².h)
Sn-9Zn	0.00006	0.556	168	$0.64.10^{-6}$
Sn-9Zn-0.5Bi	0.00008	0.35	168	$1.36.10^{-6}$
Sn-9Zn-3Bi	0.00013	0.47	168	$1.64.10^{-6}$
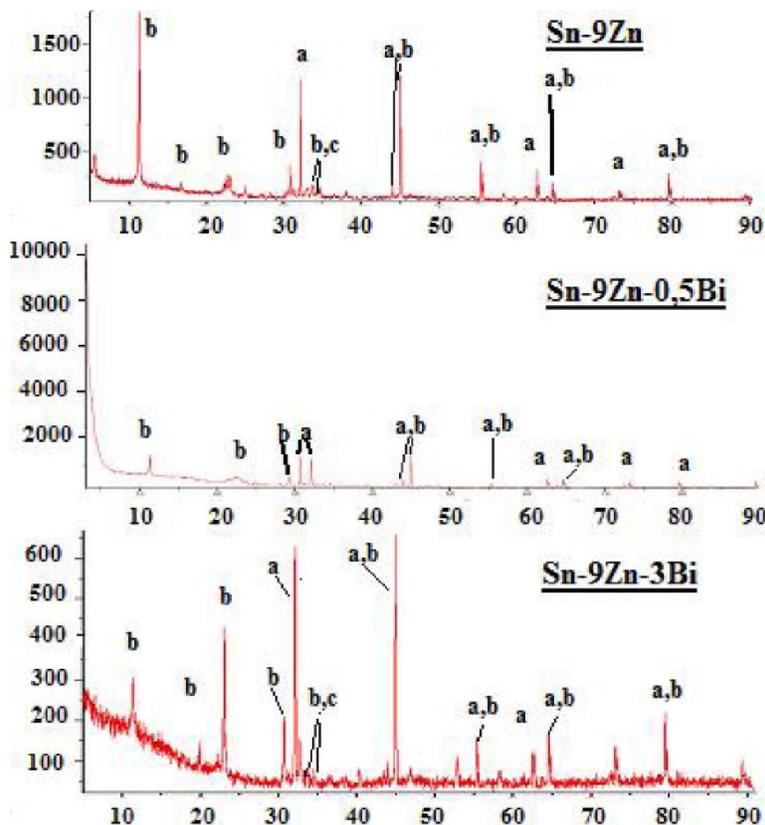
a: Sn   b: Sn-9Zn5(OH)8Cl2H2O
c: ZnO

Figure 5 : XRD spectra of our alloys after a week of immersion in NaCl 3 wt.% solution

Zinc oxide can precipitate from slightly acidic to alkaline conditions[40] i.e. it is thermodynamically stable in the general corrosive environment encountered in this work. The pH may be high enough at very active cathodic sites for zincate ions, $Zn(OH)_4^{2-}$, to form according to (6)

$$ZnO(s) \rightarrow 2OH^- + H_2O \leftrightarrow Zn(OH)_4^{2-} \qquad (6)$$
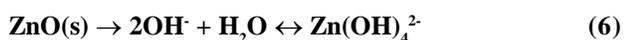
Zincate may play some role in keeping the zinc surface accessible for further oxygen reduction, thereby perpetuating corrosion. It is also possible that zinc oxide itself is sufficient catalyst for oxygen reduction due to its semi-conducting nature[41, 42].

In the presence of sodium chloride, chloride ions (Cl^-) migrate to anodic sites[43] where simonkolleite was formed according to (7)[44]:

$$5ZnO(s) + 2Cl^- + þ6H_2O \leftrightarrow$$
$$Zn_5(OH)_8Cl_2.H_2O + 2OH^- \qquad (7)$$
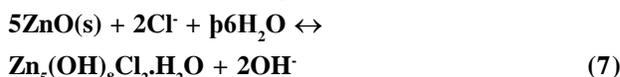
Reaction (7) shows that formation of simonkolleite releases hydroxide ions. Simonkolleite is not stable under alkaline conditions (requires pH range 6–8[43, 45]. The alkalinity associated with simonkolleite formation must be either neutralized or produced remotely from the simonkolleite. For example, alkalinity produced by simonkolleite formation at anodes can be neutralized by cathodic activity according to (6).

Full Paper

CONCLUSION

The corrosion current density (Icorr) decreases and the corrosion potential (Ecorr) increases with the Bi content in the solder from 0.5 wt.% to 3 wt.%. The addition of Bi has an important effect on the corrosion rate of Sn–9Zn. The elements of corrosion products seem provide from dissolution of zinc with formation of two compounds: ZnO and $Zn_5(OH)_8Cl_2H_2O$ in the three alloys tested.

Publication ethics

We attest that the research described in the manuscript is the original work of the author(s) that has not been previously published, in whole or in part, and that it is not under consideration by any other journal.

REFERENCES

[1]   M.Abtew, G.Selvaduray; Mater.Sci.Eng., **27**, 95 **(2000)**.

[2]   M.Mc Cormack, S.Jin; J.Electron.Mater., **23**, 635 **(1994)**.

[3]   Y.S.Kim, K.S.Kim, C.W.H.K.Suganuma; J.Alloys Compd., **352**, 237 **(2003)**.

[4]   M.Date, K.N.Tu, T.Shoji, M.Fujiyoshi, K.Sato; J.Mater.Res., **19**, 2887 **(2004)**.

[5]   A.Hirose, H.Yanagawa, E.Ide, K.F.Kobayashi; Sci.Tech.Adv.Mater., **5**, 267 **(2004)**.

[6]   K.L.Lin, L.H.Wen, T.P.Liu; J.Electron.Mater., **27**, 97 **(1998)**.

[7]   K.L.Lin, Y.C.Wang; J.Electron.Mater., **27**, 1205 **(1998)**.

[8]   K.L.Lin, L.H.Wen; J.Mater.Sci.: Mater.Electron., **9**, 5 **(1998)**.

[9]   K.L.Lin, T.P.Liu; Oxidation Metals, **50**, 255 **(1998)**.

[10] K.L.Lin, T.P.Liu; Mater.Chem.Phys., **56**, 171 **(1998)**.

[11] K.L.Lin, C.L.Shih; J.Electron.Mater., **32**, 95 **(2003)**.

[12] J.M.Song, G.F.Lan, T.S.Lui, L.H.Chen; Scr.Mater., **48**, 1047 **(2003)**.

[13] J.M.Song, T.S.Lui, G.F.Lan, L.H.Chen; J.Alloys Compd., **379**, 233 **(2004)**.

[14] M.Mc Cormack, S.Jin, H.S.Chen; J.Electron.Mater., **23**, 687 **(1994)**.

[15] R.A.Islam, B.Y.Wu, M.O.Alam, Y.C.Chan, W.Jillek; J.Alloys Compd., **392**, 149 **(2005)**.

[16] K.Suganuma; Curr.Opin.Solid State Mater.Sci., **5**, 55 **(2001)**.

[17] M.Mc Cormack, S.Jin; J.Electron.Mater., **23**, 715 **(1994)**.

[18] S.W.Yoon, J.R.Soh, H.M.Lee, B.J.Lee; Acta Mater., **45**, 951 **(1997)**.

[19] K.S.Kim, J.M.Yang, C.H.Yu, I.O.Jung, H.H.Kim, J.Alloy Compd., **379**, 314 **(2004)**.

[20] M.N.Islam,Y.C.Chana, M.J.Rizvi,W.Jillek; J.Alloys Compd., **400**, 136 **(2005)**.

[21] Chi-Chang Hu, Chun-Kou Wang; Electrochim.Acta, **51**, 4125 **(2006)**.

[22] C.Cachet, F.Ganne, S.Joiret, G.Maurin, J.Petitjean, V.Vivier, R.Wiart; Electrochim.Acta, **47**, 3409 **(2002)**.

[23] H.Park, J.A.Spuznar; Corros.Sci., **40**, 525 **(1998)**.

[24] D.Abayarathna, E.B.Hale, T.J.O'Keefe, Y.M.Wang, D.Radovic; Corros.Sci., **32**, 755 **(1991)**.

[25] R.Mayappana, A.B.Ismail, Z.A.Ahmada, T.Ariga, L.B.Hussain; J.Alloys Compd., **436**, 112 **(2007)**.

[26] P.C.Pistorius, G.T.Burstein; Corros.Sci., **38**, 525 **(1994)**.

[27] S.S.Abd EI Rehim, E.E.Fouad, S.M.Abd EI Wahab, H.H.Hassan; J.Electroanal.Chem., **401**, 113 **(1996)**.

[28] M.Windholz, S.Budavali, R.F.Blumeti, E.S.Otterbein; Merck Index, 10th Edition, (Whitehouse Station, NJ: Merck), 1257 **(1983)**.

[29] Q.Qu, L.LI, W.Bai, C.Yan, C.N.Cao; Corros.Sci., **47**, 2832 **(2005)**.

[30] N.Boshkov; Surf.Coat.Technol., **172**, 217 **(2003)**.

[31] J.B.Bajatc, V.B.M.Stankovic, M.D.Masimovic, D.M.Drazic, S.Zee; Electrochim.Acta, **47**, 4101 **(2002)**.

[32] X.G.Zhang; Corrosion and Electrochemistry of Zinc, (Plenum Press, New-York and London), 171 **(1996)**

[33] J.B.Bajat, V.B.M.Stankovic; Prog.Org.Coat., **49**, 183 **(2004)**.

[34] M.Gravilla, J.P.Millet, H.Mazille, D.Marchandise, J.M.Cuntz; Surf.Coat.Technol., **123**, 164 **(2000)**.

[35] C.Rochaix; Electrochimie, thermodynamique-cinétique, Nathan, 120 **(1996)**.

[36] M.Geary, C.B.Breslin; Corros.Sci., **39**, 1341 **(1997)**.

[37] N.C.Hosking, M.A.Strom, P.H.Shipway, C.D.Rudd; Corros.Sci, **49**, 3669 **(2007)**.

[38] M.Mouanga, P.Berçot, J.Y.Rauch; Corros.Sci, **52**, 3984 **(2010)**.

[39] M.Mouanga, P.Berçot; Corros.Sci, **52**, 3993 **(2010)**.

[40] R.Lindstrom; On the chemistry of atmospheric corrosion: a laboratory study on Zn and Mg/Mg–Al alloys, Ph.D.thesis, Goteborg University **(2001)**.

Full Paper

[41] T.Tsujimura, A.Komatsu, A.Andoh; in: Proc.Galvatech June 2001, Belgium: Stahleisen, 145 **(2001)**.

[42] T.E.Graedel; J.Electrochem.Soc., **136(4)**, 193C **(1989)**.

[43] Q.Qu, C.Yan, Y.Wan, C.Cao; Corros.Sci, **44**, 2789 **(2002)**.

[44] T.Falk, J.E.Svensson, L.G.Johansson; J.Electrochem.Soc., **145(9)**, 2993 **(1998)**.

[45] W.Feitknecht; Chemistry and Industry, **36**, 1102 **(1959)**.